Elhadj HABEL, Benyssaad KRALOUA, Ali HENNAD

Université des Sciences et de la Technologie d'Oran-Mohamed Boudiaf, USTO-MB, FGE-LMSE, BP 1505 El M'Naouer, 31000 Oran, Algeria

doi:10.15199/48.2017.05.08

Two-dimensional modeling RF glow discharge at low pressure

Abstract. *This paper presents a contribution to understand the fundamental properties of RF glow discharge based on numerical modeling. A fluid model with two dimensional based on the first three moments of Boltzmann equation, coupled with Poisson's equation is used in this work.* This equation system is written in cylindrical coordinates following the geometric shape of a plasma reactor. Our transport equation system is discretized using the finite volume approach and resolved by the exponential implicit scheme. In this work, we are used the time splitting method to resolve our system. *The model allows us to obtain the axial and radial distributions parameters of the discharge at different times of Radio-Frequency cycle (RF). The principal parameters are the electronic density, ionic density, electric potential, electric field and electronic temperature.*

Streszczenie. *W artykule analizowane jest numerycznie wyładowanie jarzeniowe RF przy niskim ciśnieniu. Wykorztano model Płynu Dwuwymiarowego oparty na pierwszych trzech momentach w rówananiu Boltzmanna, w połączeniu z równania Poissona. Ten układ równań opisana we współrzędnych walcowych w reaktorze plazmowym. Określono główne parametry gęstości elektronowej, gęstości jonowej, potencjał elektryczny, pole elektryczne.* ***Dwuwymiarowe modelowanie wyładowania jarzeniowego RF przy niskim ciśnieniu)***

Keywords: RF glow Discharge, Fluid Model, charged particle transport, time splitting method.
Slowa kluczowe: wyładowanie jarzeniowe RF, model cieczy, metoda dzielenie czasu

Introduction

RF glow discharges are used in a wide variety of applications in modern science and technology [1]. One of the largest and most important fields of application is the microelectronics industry, where RF glow discharges are used for etching of surfaces to form topographical surface features, as well as for depositing thin films. Similarly, glow discharges are used extensively in the materials processing industries for deposition of various thin films, coatings, and surface layers, and may additionally be employed for surface cleaning, pretreatment, and modification processes. Our model is based on the first three moments of Boltzmann's equations for ions and electrons, coupled to Poisson's equation. By considering the geometry of a plasma reactor, the transport equations are written in cylindrical coordinates.

In this work, we consider that RF glow discharge arises between two metal electrodes circular, plane and parallel. The two-dimensional transport equations are transformed into one-dimensional equations (drift-diffusion equation), while a time splitting approach [8,9] is adopted.

Model formulation

In this work, the model used to describe the kinetics of the charged particles for the RF glow discharge is the second order fluid model. It is based on the first three momentums resolution of the Boltzmann equation. These three moments are continuity, momentum transfer and energy equations, which are strongly coupled with the Poisson's equation by considering the local electric field approximation for ions and the local mean energy approximation for electrons.

In the present model, the transport equations derived from the first three moments of Boltzmann's equation are written only for electrons and positive ions.

The two-dimensional equations of the electron and positive ion density are described by continuity equations expressed in cylindrical geometry [7,8,9,10].

$$\frac{\partial n_e}{\partial t}+\frac{\partial \Phi_{ez}}{\partial z}+\frac{1}{r}\frac{\partial\left(r\Phi_{er}\right)}{\partial r}=S_e \tag{1}$$

$$\frac{\partial n_+}{\partial t}+\frac{\partial \Phi_{+z}}{\partial z}+\frac{1}{r}\frac{\partial\left(r\Phi_{+r}\right)}{\partial r}=S_+ \tag{2}$$

In the model, the momentum conservation equation is replaced by the drift-diffusion approximation; hence, the transport equation is represented by two separate terms, drift and diffusion terms [4]. The electron and ion density fluxes are given by the following expression:

$$\Phi_{ez}=-\mu_e n_e E_z-D_e\frac{\partial n_e}{\partial z} \tag{3}$$

$$\Phi_{er}=-\mu_e n_e E_r-D_e\frac{\partial n_e}{\partial r} \tag{4}$$

$$\Phi_{+z}=+\mu_+ n_+ E_z-D_+\frac{\partial n_+}{\partial z} \tag{5}$$

$$\Phi_{+r}=+\mu_+ n_+ E_r-D_+\frac{\partial n_+}{\partial r} \tag{6}$$

In the source term, only the ionization is considered, and other reactions are neglected, because we think that ionization is the main process in the RF glow discharge [2,12].

The source term S_e and S_+ are expressed as a function of the electron temperature T_e in an Arrhenius form as shown [3,12].

$$S_e=S_+=k_i N n_e\, exp(-E_i / K_b T_e) \tag{7}$$

Where k_i is the pre-exponential coefficient, E_i is the ionization activation energy, N is the density of the neutral gas and K_b is the Boltzmann constant.

The electron temperature is calculated by the energy electron equation given by:

$$\frac{\partial n_\varepsilon}{\partial t}+\frac{\partial \Phi_{\varepsilon z}}{\partial z}+\frac{1}{r}\frac{\partial\left(\Phi_{\varepsilon r}\right)}{\partial r}=S_\varepsilon \tag{8}$$

where $n_\varepsilon=n_e\varepsilon_e$ is the electron energy density and Φ_ε is the electronic energy density flux.

The flux of electron energy density can be written as:

$$\Phi_{\varepsilon z}=-\frac{5}{3}n_\varepsilon\mu_e E_z-\frac{5}{3}D_e\frac{\partial n_\varepsilon}{\partial z} \tag{9}$$

(10) $$\Phi_{\varepsilon r} = -\frac{5}{3} n_{\varepsilon} \mu_e E_r - \frac{5}{3} D_e \frac{\partial n_{\varepsilon}}{\partial r}$$

The source term S_{ε} is represented by two terms, an ohmic heating term and a collision loss term given by:

(11) $$S_{\varepsilon} = -e\Phi_e E - \sum_j S_j H_j$$

where the summation is over the reactions involving inelastic electron collisions and H_j is the electron energy loss per collision. This summation included ionization and excitation. Where the term excitation is given by:

(12) $$S_{ex} = k_{ex} N n_e \exp(-E_{ex} / K_b T_e)$$

Poisson's equation is resolved in cylindrical geometry for the determination of the electric field and the discharge potential.

(13) $$\frac{\partial^2 V}{\partial z^2} + \frac{1}{r}\frac{\partial V}{\partial r} + \frac{\partial^2 V}{\partial r^2} = \frac{e}{\varepsilon_0}(n_e - n_+)$$

where, V is the electric potential, e is the elementary charge, and ε_0 is the permittivity of free space.

The axial E_z and radial E_r components of the electric field strength are then found from the partial derivatives of the potential function, and are given by

(14) $$E_z = -\frac{\partial V}{\partial z} \quad \text{and} \quad E_r = -\frac{\partial V}{\partial r}$$

Boundary conditions

The use of boundary conditions for the above mentioned transport equations is essential for the description of our problem.

In the model, boundary conditions were as follows:

At $z = 0$ (surface of left electrode)

(15) $$V = -V_{rf} \sin\left(2\pi f t\right)$$

(16) $$\Phi_e = -\gamma \Phi_+$$

(17) $$\frac{\partial n_+}{\partial z} = 0$$

(18) $$T_e = T_{ec}$$

At $z = L$ (surface of right electrode)

(19) $$V = 0$$

(20) $$\Phi_e = -\gamma \Phi_+$$

(21) $$\frac{\partial n_+}{\partial z} = 0$$

(22) $$T_e = T_{ec}$$

Here, γ is the secondary electron emission coefficient, V_{rf} is the peak radio-frequency voltage, L is the inter-electrodes spacing and f is the excitation frequency. The boundary conditions on the electron temperature is difficult to specify [11]. A simplified constant temperature condition was used in the present study.

At the symmetrical axis and the dielectric wall, we used mainly Neumann boundary conditions:

$\frac{\partial n_e}{\partial r} = 0$ and $\frac{\partial n_+}{\partial r} = 0$ for the gradient particle densities, $\frac{\partial V}{\partial r} = 0$ for the electric potential and $\frac{\partial T_e}{\partial r} = 0$ for the electron temperature.

The boundary conditions used in our 2D model are recapitulated in Fig.1.

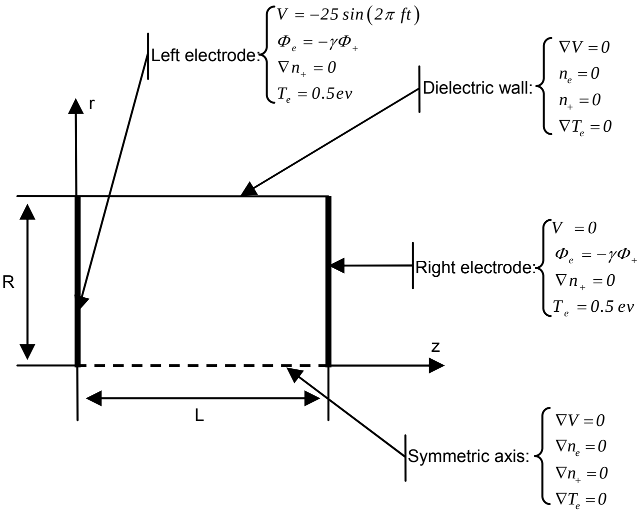

Fig.1: Schematic representation of the boundary conditions used in our 2D model.

Numerical methods

The problem consists of determining the electron and positive ion density, electric potential, electric field and electron temperature as function of axial and radial position at different times of radio-frequency cycle.

For the charged particles, equations (1) and (2) have to be solved. Equation (8) for electron energy has the same form, by changing particle density n_e with electron mean energy density n_{ε} and correctly expressing the source term S_{ε}. Thus the resolution of the transport equations is done in the same way.

Thus the form of the transport equation to be solved is expressed in cylindrical geometry as follows:

(23) $$\frac{\partial n}{\partial t} + \frac{\partial \Phi_z}{\partial z} + \frac{1}{r}\frac{\partial\left(r\Phi_r\right)}{\partial r} = S$$

In this work, we use the method of the fractional steps [12] to solve the equation (23). This method consists in replacing the two-dimensional equations by a system of one-dimensional equations in the object to reduce considerably the calculation time in each direction of space.

(24.a) $$\frac{\partial n}{\partial t} = S$$

(24.b) $$\frac{\partial n}{\partial t} + \frac{\partial \Phi_z}{\partial z} = 0$$

(24.c) $$\frac{\partial n}{\partial t} + \frac{1}{r}\frac{\partial\left(r\Phi_r\right)}{\partial r} = 0$$

The discretization method of the equations system above is based on the finite difference scheme.

The system of equations becomes:

(25.a) $$\frac{n_{i,j}^{m+1} - n_{i,j}^{m}}{\Delta t} = S_{i,j}$$

(25.b) $$\frac{n_{i,j}^{m+1} - n_{i,j}^{m}}{\Delta t} + \frac{\Phi_{i+1/2,j} - \Phi_{i-1/2,j}}{\Delta z} = 0$$

(25.c) $$\frac{n_{i,j}^{m+1}-n_{i,j}^{m}}{\Delta t}+\frac{\Phi_{i,j+1/2}-\Phi_{i,j-1/2}}{\Delta r}=0$$

The drift-diffusion fluxes are discretized using the Scharfetter-Gummel exponential scheme [6].

(26) $$\Phi_{i+1/2,j}=\frac{D}{\Delta z}\left(\frac{R_1}{1-exp(R_1)}n_{i+1,j}-\frac{R_1\,exp(R_1)}{1-exp(R_1)}n_{i,j}\right)$$

(27) $$\Phi_{i-1/2,j}=\frac{D}{\Delta z}\left(\frac{R_2}{1-exp(R_2)}n_{i,j}-\frac{R_2\,exp(R_2)}{1-exp(R_2)}n_{i-1,j}\right)$$

(28) $$\Phi_{i,j+1/2}=\frac{D}{\Delta r}\left(\frac{R_3}{1-exp(R_3)}n_{i,j+1}-\frac{R_3\,exp(R_3)}{1-exp(R_3)}n_{i,j}\right)$$

(29) $$\Phi_{i,j-1/2}=\frac{D}{\Delta r}\left(\frac{R_4}{1-exp(R_4)}n_{i,j}-\frac{R_4\,exp(R_4)}{1-exp(R_4)}n_{i,j-1}\right)$$

Where:

$$R_1=\mu\frac{E_{i+1/2,j}}{D}\Delta z\ ,\quad R_2=\mu\frac{E_{i-1/2,j}}{D}\Delta z\ ,$$

$$R_3=\mu\frac{E_{i,j+1/2}}{D}\Delta r\ ,\quad R_4=\mu\frac{E_{i,j-1/2}}{D}\Delta r$$

Many numerical techniques exist for the solution of such sets of two-point equations, varying in their efficiency and simplicity. In this work, we used the Thomas algorithm to calculate the density $n_{i,j}^{m+1}$.

The Poisson's equation (13) is most often discretized by using central finite-difference scheme.

With: $$\begin{cases}\dfrac{\partial^2 V}{\partial z^2}=\dfrac{V_{i-1,j}-2V_{i,j}+V_{i+1,j}}{\Delta z^2}\\[2mm] \dfrac{\partial^2 V}{\partial r^2}=\dfrac{V_{i,j-1}-2\ V_{i,j}+V_{i,j+1}}{\Delta r^2}\\[2mm] \dfrac{\partial V}{\partial r}=\dfrac{V_{i,j+1}-V_{i,j-1}}{2\,\Delta r}\end{cases}$$

The resolution of the Poisson's equation is solved using iterative methods from the Successive Over-Relaxation (SOR) combined by Thomas algorithm for the tridiagonal matrix [5].

Results and discussions

An argon-like discharge was studied as an example of an electropositive discharge.

The following table gathers all the source data and the transport parameters used in our two dimensional modeling.

Fig.2 shows the electron and ion densities distribution in the gap on the symmetric axis (r=0 cm) for 25% and 75% of radio-frequency cycle. At 25% RF cycle, the left electrode is at its peak negative potential. The electron density is modulated substantially near the electrodes, with the electrons repelled by the momentary cathode and attracted by the momentary anode (at 75% RF cycle, left electrode). However electron density profiles wich are flatter in the bulk (plasma) can be obtained by increasing the gas pressure or the electrode spacing.

The ion density is not modulated by the RF since the ions are too massive to respond to the rapidly changing field.

Table.1: Transport parameters and operating conditions used in the present simulation [13].

Symbol	Value
$L(cm)$	3.0
$R(cm)$	4.0
$P(torr)$	1.0
$V_{rf}(V)$	25
$f\ (MHz)$	10
$T_{gaz}(K)$	273
$ND_e(cm.s)^{-1}$	1.7×10^{22}
$ND_+(cm.s)^{-1}$	8.0×10^{17}
$N\,\mu_e(V.cm.s)^{-1}$	8.5×10^{21}
$N\,\mu_+(V.cm.s)^{-1}$	3.6×10^{19}
$k_i(cm^3/s)$	1.0×10^{-7}
$E_i(eV)$	17.7
$H_i(eV)$	17.7
$k_{ex}(cm^3/s)$	5.0×10^{-9}
$E_{ex}(eV)$	11.6
$H_{ex}(eV)$	11.6
γ	0.05
$T_{ec}(eV)$	0.5

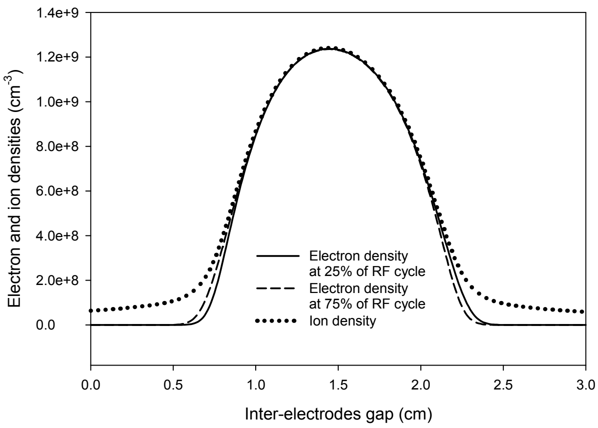

Fig.2: Electron and ion densities on the symmetric axis at 25% and 75% RF cycle.

The electric potential and electric field distribution in the gap are shows in Fig.3 and Fig.4. The potential oscillates according to the applied sinusoidal waveform, at the left electrode (z=0 cm), while the right electrode (z=3 cm) is always at ground (zero) potential. The potential of the plasma is seen to be more positive than the potential of either electrode at any time of RF cycle.

The potential drop in the plasma is comparatively small, since the mobile electrons provide for a high conductivity in the bulk. However, a sharp potential drop is seen in the plasma sheath, especially when the electrode is the momentary cathode (25% RF cycle at z=0 cm, and 75% RF cycle at z=3 cm).

The electric field is rather weak in the pulk plasma, since the plasma is a nearly equipotential volume. However, relatively strong electric fields develop in the sheath, and the sheath electric field is severely modulated by the RF.

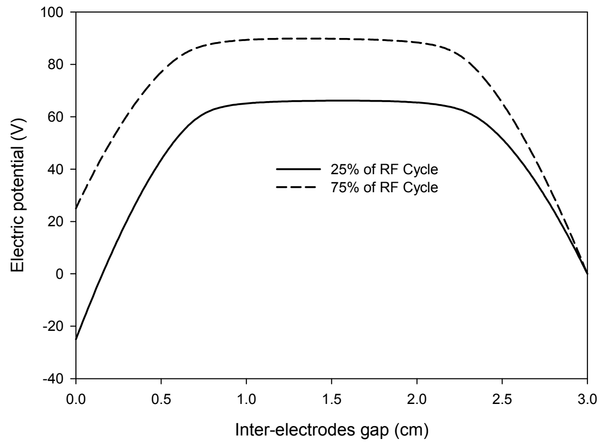

Fig.3: Electric potential on the symmetric axis at 25% and 75% RF cycle.

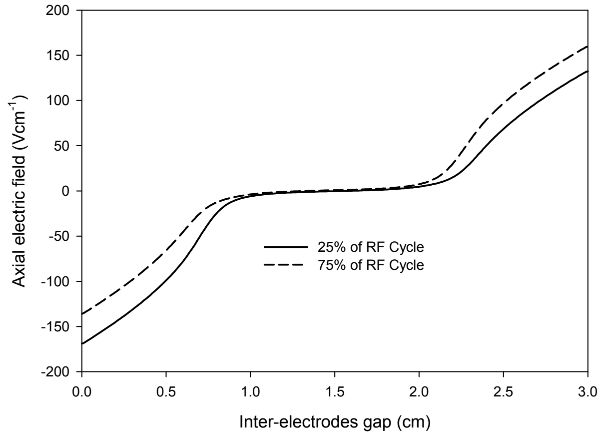

Fig.4: Axial electric field on the symmetric axis at 25% and 75% RF cycle.

Fig.5 shows the electron temperature distribution in the gap at 25% and 75% RF cycle. We observe much higher temperatures near the plasma-sheath interface during the cathodic part of the RF cycle, since the presence of the relatively intense electric field. In the plasma electron temperature is lower and nearly time independent.

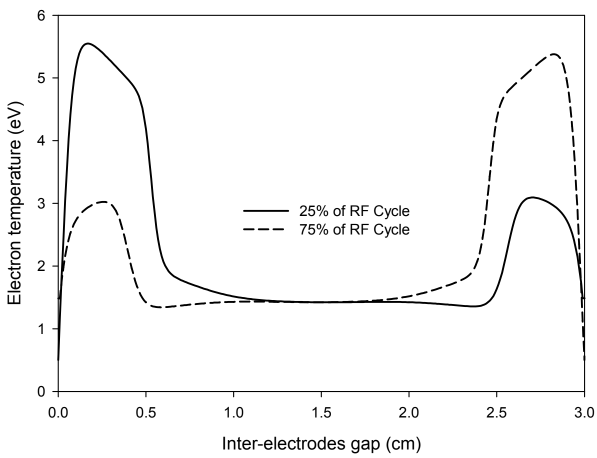

Fig.5: Electron temperature on the symmetric axis at 25% and 75% RF cycle.

Figs.6, 7 and 8 represent the distribution axial and radial of charged particle at 25% and 75% RF cycle. The 2D distribution of electric potential, axial and radial electric field at 25% and 75% RF cycle are shows respectively in figs.9, 10, 11, 12, 13 and 14.

Figs.15 and 16 are the plot 2D of electron temperature at 25% and 75% of the RF cycle.

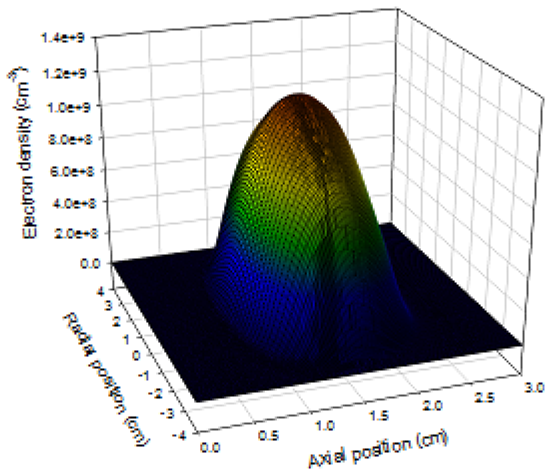

Fig.6: 2D distribution of electron density at 25% RF cycle.

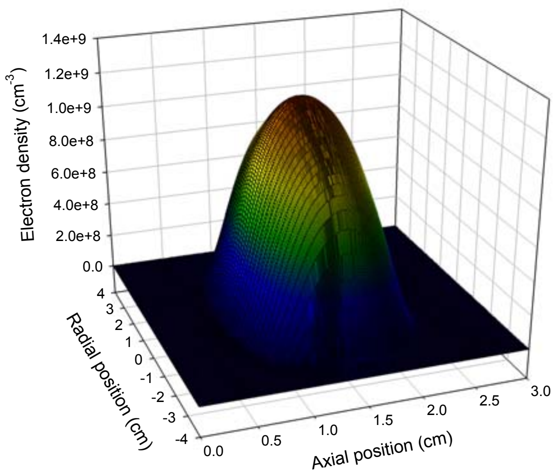

Fig.7: 2D distribution of electron density at 75% RF cycle.

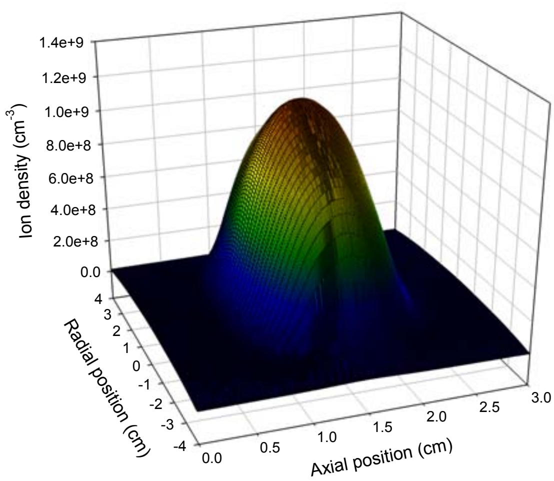

Fig.8: 2D distribution of ion density at 25% and 75% RF cycle.

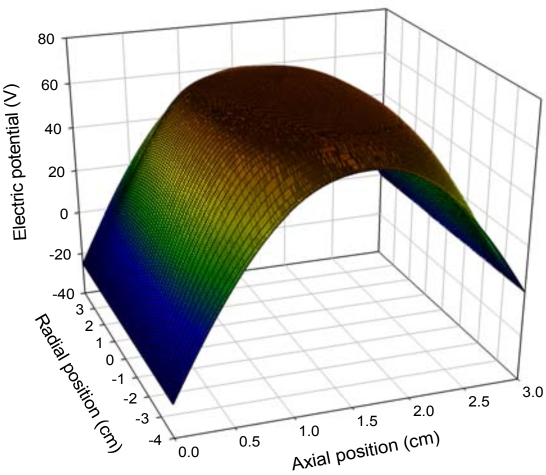

Fig.9: 2D distribution of electric potential at 25% RF cycle.

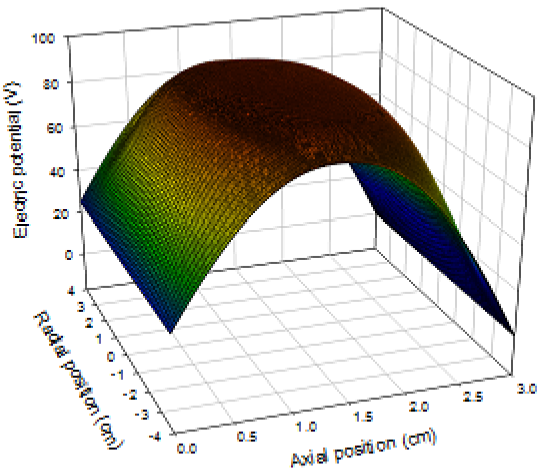

Fig.10: 2D distribution of electric potential at 75% RF cycle.

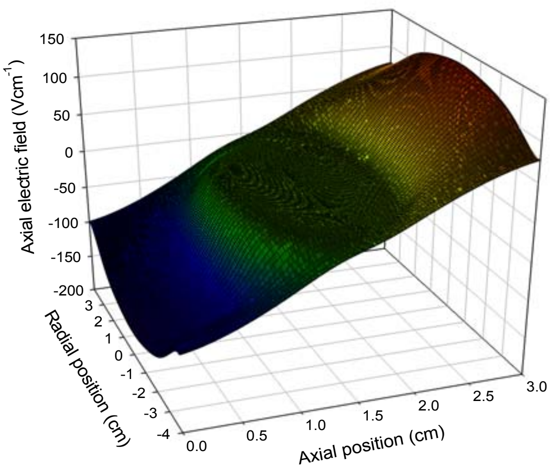

Fig.11: 2D distribution of axial electric field at 25% RF cycle.

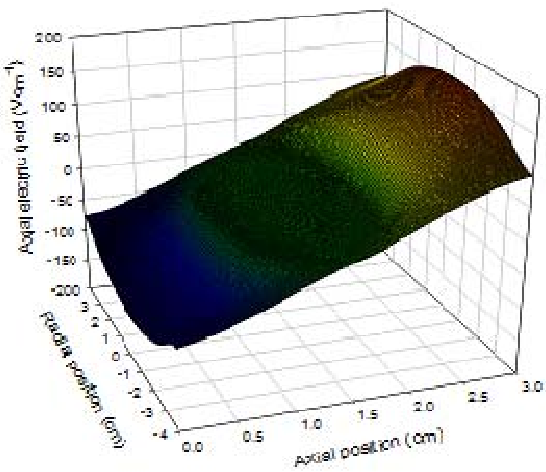

Fig.12: 2D distribution of axial electric field at 75% RF cycle.

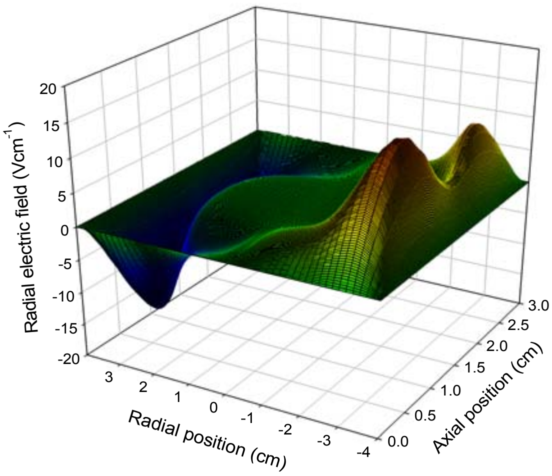

Fig.13: 2D distribution of radial electric field at 25% RF cycle.

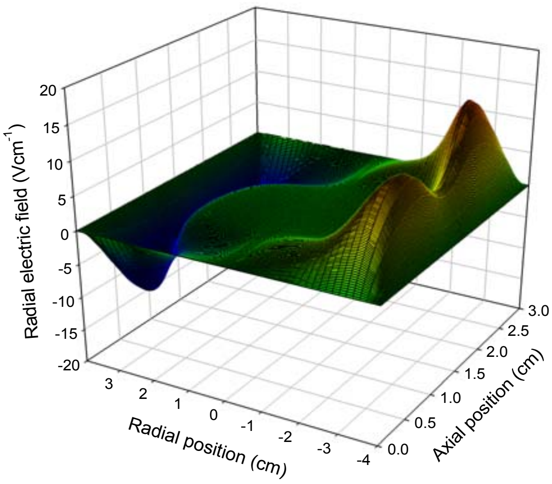

Fig.14: 2D distribution of radial electric field at 75% RF cycle.

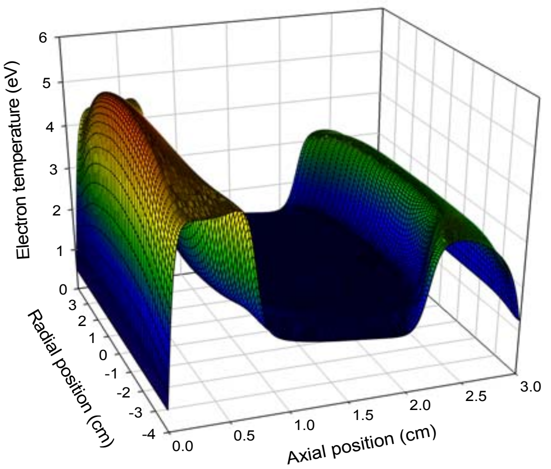

Fig.15: 2D distribution of electron temperature at 25% RF cycle.

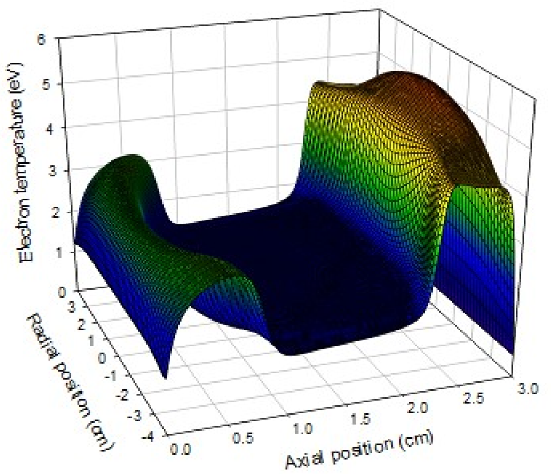

Fig.16: 2D distribution of electron temperature at 75% RF cycle.

Conclusion

In this paper, a fluid model with two dimensional was used to analyse charged particle transport in low pressure radio-frequency (RF) discharges. The algorithm based on finite difference method for the spatial and radial discretization coupled to the time splitting technical. This technical is a good approach to resolve the two-dimensional transport equation of the radio-frequency glow discharge model. An argon-like discharge was examined as an example of an electropositive discharge.

Nomenclature

n_e, n_+ and n_ε	Electron, ion and energy number density
Φ_e, Φ_+	Electron and Ion flux
S_e, S_+ and S_ε	Source term for Electron, ion and energy
V	Electric potential
E	Electric field
ε_e	Electron energy
T_e	Electron temperature
μ_e, μ_+	Electron and Ion Mobility
D_e, D_+	Electron and ion diffusivity
γ	Coefficient for secondary electron emission
N	Neutral species density
e	Elementary charge
ε_0	Free space permittivity
L	Longitudinal inter-electrode gap
R	Radius of the electrodes
Δz	Axial spatial step
Δr	Radial spatial step
Δt	Temporal step
T	Period

Authors

ElHadj Habel was born in Tissemsilt, Algeria, on April, 02, 1979. His scientific interests include the theoretical study and modeling of physical processes in gas discharge plasma. E-mail: hadj.habel@usto-univ.dz

Ali Hennad was born in Oran, Algeria, on January, 27, 1964. He received the PH.D degree with a thesis on the kinetics of ions in molecular gases to determine ion basic data in air form Monte Carlo simulation, University Paul Sabatier of Toulouse, France in 1996. He is currently a Professor at University of Sciences and Technology of Oran, Algeria. His field of expertise is more particularly the modeling of the electric and hydrodynamic behaviors of the plasmas generated in low and high pressure. He has also a good expertise on the numerical analysis of the nonlinear and strongly coupled elliptic transport equations, and the swarm parameters determination of the charged particles in no equilibrium reactive plasma. He is the author of various international publications, a lot of them in collaboration with the LAPLACE Laboratory, Toulouse, France.
E-mail: ali.hennad@gmail.com

REFERENCES

[1] A. Bogaerts, The glow discharge: an exciting plasma, J. Anal. At. Spectrom. 14 (1999) 1375–1384

[2] Yu Qian, Deng Yong Feng, Numerical study on characteristics of argon-radiofrequency glow discharge with varying gas pressure, Chin.Phys.Lett. Vol. 25(2008), No. 7,2569

[3] M.H. Elghazaly, S. Solyman, Electron impact ionization and excitation rate coefficients in the negative glow region of a glow discharge, journal of Quantitative Spectroscopy & radiative Transfert 103(2007),260-271

[4] B. Kraloua, A. Hennad, Multidimentional numerical simulation of glow discharge by using the N-BEE-Time splitting method, *Plasma Science and Technology*, Vol.14, Sep(2012), No.9

[5] A. Luque, U. Ebert, Densitymodels for streamer discharges: Beyond cylindrical symmetry and homogeneous media, Journal of Computational Physics 231 (2012) 904-918

[6] L. Scharfetter, H. K. Gummmel, *IEEE Trans. Electron Devices,* 64(1969), No.16

[7] M. Meyyappan, J P. Kreskovsky, J. Appl. Phys ,68, 1506, 1990

[8] C. Lee, D.B. Graves, M.A. Lieberman, et al. 1994, J.Electrochem, Soc., 141: 1546

[9] I. Lee, D.B. Graves, Lieberman M A. 2008, Plasma Sources Sci. Technol. 17: 015018

[10] N. Benaired, A. Hennad, ADBQUICKEST Numerical Scheme for Solving Multi-Dimensional Drift-Diffusion Equations, PRZEGLĄD ELEKTROTECHNICZNY, ISSN 0033-2097, R. 90 NR 8/2014

[11] D. B, Graves, J. Appl. Phys. 62,88 (1987).

[12] H. Tebani, A. Hennad, three-dimensional modelling of the DC glow discharge using the second order fluid model, PRZEGLĄD ELEKTROTECHNICZNY, ISSN 0033-2097, R. 89 NR 8/2013

[13] Sang-Kyu Park and Demetre J. Economou . Appl. Phys. 68, 3904 (1990).